# JANOS

**Blue Team Members:**
Jonatan Adolfsson, Laura Antoni-Micollier, Nikolaus Walter Bucheim, Paolo Cappuccio, Silvio De Carvalho, Vittorio De Falco, Nina Fleischmann, Nicolas Gampierakis, Samuel Góngora Garcia, Matthieu Laporte, Neda Meshksar, Mihaela Nastase, Timo Nikkanen, Sam Pallister, Luisa Santo

**Team Tutors:**
Günter Kargl and Oliver Jennrich

Abstract

*While various facets of quantum mechanics are being addressed with particle physics experiments on ground, experiments in space are dedicated testing aspects of general relativity. However to date, no attempt has been made to address the interplay of general relativistic and quantum effects in one experiment.*
*To close this gap, we propose* JANOS *- an experiment designed to examine the effect of gravity on quantum systems. The basis of the experiment is a single-photon interferometer, distributed between an Earth orbiter and a ground station; the photons are split in a superposition to explore how gravity acts on them, compared to a classical system. Therefore we aim at confirming, or refuting, the hypothesis that there is a fundamental effect of gravity on quantum systems.*

**Mission Target:**
Eccentric polar orbit around the Earth
**Duration:**
2 years
**Mission Class**
M - €583M

## Scientific Background

The universe as we know it is underpinned by two theoretical frameworks, both developed in the early stages of the twentieth century. On the one hand, Einstein's general theory of relativity (GR) describes the physics of gravity and is the basis of our entire contemporary understanding of cosmology. On the other hand, quantum mechanics (developed by physicists including Schrödinger, Heisenberg, Bohr and Dirac) describes the physics of the very small; without it, we would have no understanding of nuclear physics, particle physics or solid-state physics.

Both of these theories have been extensively explored in isolation, and it is a real testament to their robustness that they remain correct even when probed in the exquisite detail achievable by contemporary experiments. Regarding general relativity, tests include probing the equivalence principle (the weak formulation of which has been tested to an accuracy of $10^{-13}$ [1]) and tests of the Shapiro delay (the slowing of light as it passes by a massive body; acutely measured by radio links with the Cassini spacecraft). Regarding quantum mechanics, quantum descriptions of particle physics have now been verified to an accuracy of $10^{-8}$ with ground-based atomic physics experiments.

In stark contrast to the success of these theories, we also know the following: quantum mechanics and general relativity are fundamentally incompatible. Naïve attempts to combine them into a full theory of "quantum gravity" give nonsensical answers. As such, the primary goal of theoretical physics for the last half century has been to discover the underlying theory that unites general relativity and quantum mechanics. Proposals for theories of quantum gravity often make predictions that deviate marginally from what can be expected with established theories, and so the tests mentioned above are designed to rule out potential candidates for theories of quantum gravity in addition to probing the accuracy of general relativity and quantum mechanics.

To date, all experimental explorations of quantum gravity have been tests of general relativity or quantum mechanics, in isolation. Advances in control of individual quantum systems mean that regimes can be explored where both the quantum nature of matter and general relativity are working in tandem. The proposal herein aims to be the first experiment ever carried out

in a regime where both quantum mechanics and GR are important dynamically. Confirmation or refutation of our scientific hypothesis (to be presented in more detail below) will have a deep impact on the course of theoretical physics in the 21st century.

## Scientific Objectives

The goal of this mission is to test to a statistical significance the hypothesis: that a single, purely quantum system evolves under gravity in the same way as classical light. To this end, we propose the following scientific objective:

**SO1: Test whether single photons are affected by GR in the same way as classical light.**

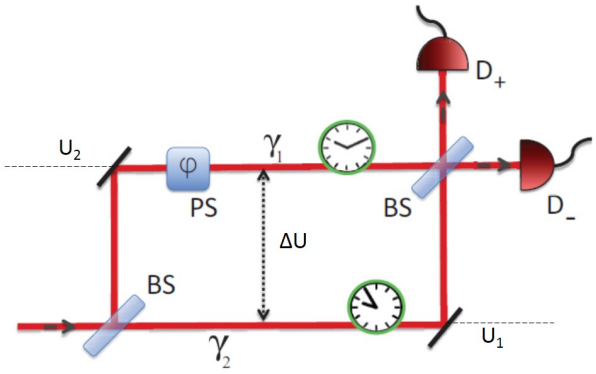


Figure 1: A cartoon of the interferometric setup. Photons are split at a beamsplitter into a superposition of two paths. Then, one arm is transmitted to a higher gravitational potential. GR implies a time delay between the arms, which can be detected at the output. From [2].

We propose to do this using single-photon interferometry; explicitly, we consider preparing a superposition of two spatially seperated parts, such that each of the parts experiences a different flight time due to the Shapiro delay. The Shapiro delay is a strictly general relativistic effect, and has no analogue in Newtonian gravity. Therefore one part of the single-photon wavefunction would "lag" behind the other due to general relativistic effects, which can be detected using conventional optics. A schematic of the proposed experiment is shown in Figure 1, and the predicted behaviour for two different example altitudes is shown in Figure 2. The additional phase, $\Delta\phi_G$, is present in both Newtonian gravity and general relativity, whereas the drop in fringe contrast is a strictly non-Newtonian effect. The predicted drop in fringe contrast is given by [2]:

$$V = \exp\left[\left(\frac{\Delta\tau}{2\sqrt{\sigma}}\right)^2\right], \qquad (1)$$

where $\Delta\tau$ is the Shapiro delay and $\sqrt{\sigma}$ is the photon coherence time.

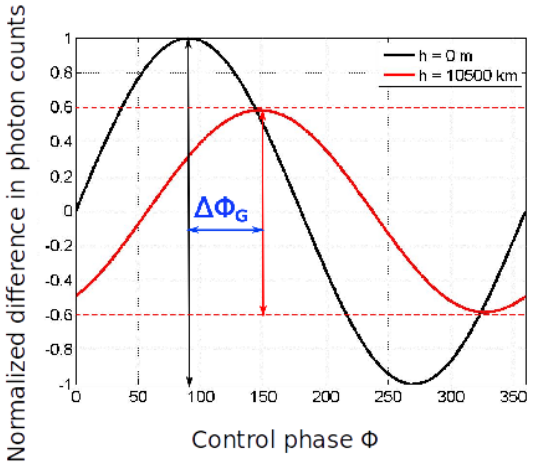


Figure 2: An example of interference fringes for a pair of satellite heights. $\Delta\phi_G$ is present in both the Newtonian and relativistic case, whereas the drop in contrast with altitude is exlusively relativistic.

### Measurement Strategy

Completing objective **SO1**, by observing the drop in fringe contrast, requires tracing out enough of the interference pattern that the contrast can be estimated with high confidence. Therefore we include a preliminary science requirement:

**SR1: Measure a full interference fringe for each altitude bin.**

This also immediately leads to a subsidiary objective because it also provides an additional test:

**SO2: Test whether single photons couple to *Newtonian* gravity in the same way as classical light.**

A controllable phase delay in one of the arms of the interferometer will be included to trace out this interference pattern, implemented by a waveguide electro-optic modulator (EOM). We will then repeatedly vary the phase from 0 to $2\pi$ to record a full interference fringe. This measurement will be repeated many times in a given interval of orbit altitude. Depending on the altitude the fringe pattern should shift by a certain amount [2]:

$$\Delta\phi_G = \frac{2\pi l}{\lambda}\frac{\Delta U}{c^2}, \qquad (2)$$

where $l$ is the fibre length, $\lambda$ the wavelength and $\Delta U$ the change in gravitational potential.

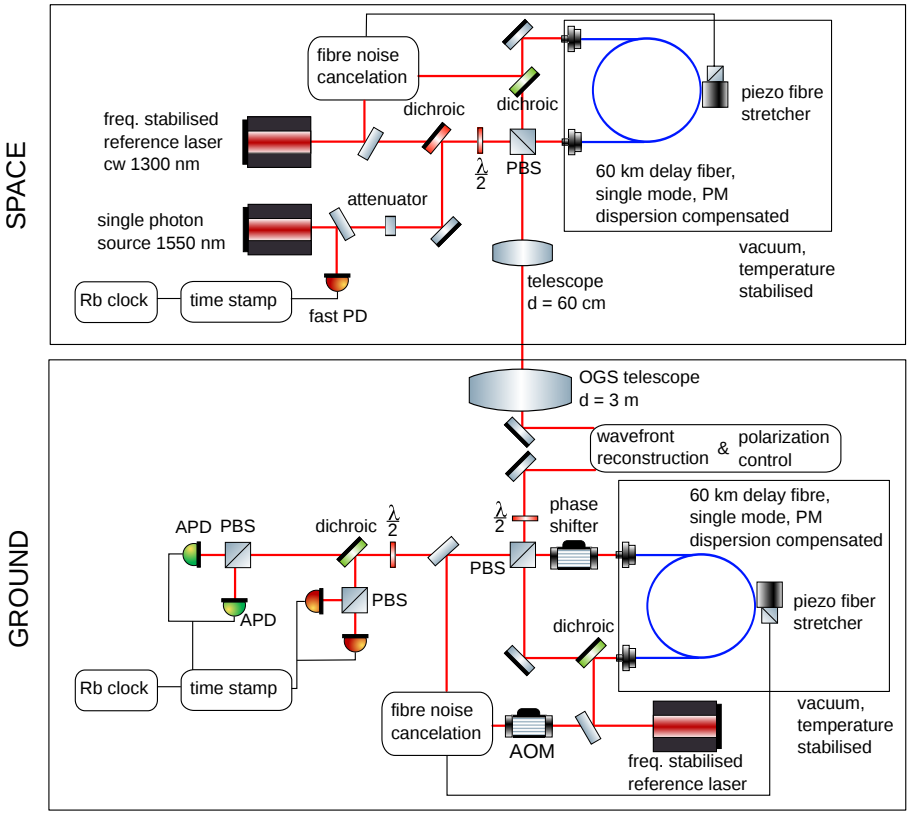


Figure 3: A full schematic of the payload optical system.

### Scientific Requirements

The only other scientific requirement for the proposed mission is to provide the necessary measurement accuracy and total photon count in order to unambiguously test the above stated hypothesis. We demand the following scientific requirement on the coefficient of variation of the fringe contrast (the ratio of the contrast error to the mean contrast):

**SR2: Collect enough data to establish a coefficient of variation less than $\frac{1}{5}$.**

This $5\sigma$ precision is common for hypothesis testing and is ubiquitous in experiments in particle physics and astronomy.

## Payload Requirements

A detailed illustration of the interferometer setup can be seen in Figure 3. A short overview of the key elements will be presented below. The single photon pulses will be tagged with timestamps by a Rb-clock (chosen primarily for its small size, weight and commercial availability). Synchronization with an identical clock on the ground will be used to exclude background noise at the data post-processing stage. Precision timing is also necessary to modulate the action of time-gate filters in front of the detectors. Alongside the single-photon source, a frequency stabilised reference laser will be guided through the interferometer. The fibres will be kept in a temperature stabilized environment to minimize length and phase fluctuations. On the ground station, a fraction of the incident laser power will be separated and used for wavefront reconstruction and compensation of polarization changes due to satellite movement. Additionally, both the satellite and the ground station will include a feedback loop of a frequency stabilized reference laser in combination with a piezo fibre stretcher, which will allow for fibre noise reduction and stabilisation of the interferometer.

Critical instrument requirements for the JANOS mission can only be stated based on a measurement strategy that takes into account technology readiness and the various limiting factors of a satellite based quantum optics experiment. The functional dependence of the desired drop in fringe contrast (see Formula 1 and Figure 2) on the experimental parameters ($\Delta\tau$ and $\sqrt{\sigma}$) commands the following reasoning:

- Utilization of ultrashort ($< 1ps$) single photon pulses to increase the observable decoherence effect.
- Optimisation of the satellite orbit with respect to single photon link efficiency, drop in fringe contrast and total measurement time.

- Mitigation of large dispersion by statistical averaging.

In order to optimize these parameters with regard to the scientific requirements, we estimate a requirement on the total number of measurements of $7 \times 10^7$ with a single photon count rate greater than 100 cps. This infers the following instrumental requirements:

- Single photon coherence time less than $4ps$, resulting in a drop of fringe contrast of 0.17% between perigee and apogee.
- Fiber dispersion $< 5fs/km/nm$, ensuring a broadening of the pulse width in the fibres of $< 0.5\%$ per km.
- Relative optical path length stability of the interferometer less than $10^{-10}$.
- Relative frequency stability of the reference laser less than $10^{-11}$ to ensure interferometer stabilisation.
- Temperature stabilisation of the fibres of less than $10^{-3}$K to ensure interferometer stabilisation.

Meeting these requirements provide a range of challenges. We highlight particularly the fiber dispersion of $5fs/km/nm$ as a loss leader. The current state-of-the-art for dispersion-limited fiber is a factor of ten worse than this: $50fs/km/nm$ [3]. However, we include research and development costs in the budget calculations.

## Key Optical Elements

*Single photon source:* To observe a quantum mechanical effect the interference of single photons is crucial. An off-the-shelf mode-locked pulsed laser with operation wavelength of 1550 nm and 1 GHz repetition rate will be attenuated to a mean photon number of 0.1 photons per pulse. The reason for this particular level of attenuation is to reduce the probability of multiphoton emission to 5% and results in a single photon rate of 100 MHz, which matches the resolution of the single photon detectors. The chosen wavelength guarantees high atmospheric transmission and the utilization of well developed telecommunication technology.

*Classical reference laser:* A 1300 nm multi-purpose laser, operating in continuous wave mode, will be led alongside the single photons through the interferometer. It will provide reference data, that will help to estimate phase fluctuations and systematic errors. It will also be employed as a comparison of the "classical" fringe contrast to the "quantum" fringe contrast. For precise corrections, an operational wavelength as close as possible to the single photons is required, but overlap with the bandwidth of the single photon pulses has to be avoided. The chosen wavelength is a reasonable compromise. To meet the scientific requirements a relative frequency stability of $10^{-11}$ is required. This can be achieved by multiple established technologies, such as stabilizing it to an atomic or molecular absorption line using high precision cavities or frequency combs.

*Fibres:* The delay fibres need to be stabilised to relative length changes of $10^{-10}$ for observing the predicted interference effects, which includes a thermal stabilisation of $\pm 10^{-5}$K and active length corrections by a piezo fibre-stretcher.

*Transmission telescope:* The onboard emitting telescope will be used to focus the beam coming from the two different sources. It will be a 60 cm aperture, 1 m long, 6 $\mu$rad FOV Cassegrain reflector telescope. The mirrors will be made out of Beryllium to limit its weight.

*Single-photon detectors:* The single photon detectors will be a pair of four multiplexed single-nanowire single-photon detectors (SNSPDs), to benefit from the superior dark count over conventional APDs. The technology has already been established in the LADEE mission (NASA).

## Technological Readiness

Current technologies are capable of dispersion compensation in optical fibres of $0.5ps/km/nm$, which has to be improved about a factor of ten to make the scientific requirement feasible. However, the utilization of telecommunication fibre wavelengths ensure ongoing research in that scientific area.

Long term accuracy of the reference laser within required precision is today only feasible via frequency comb stabilization. This method will increase further complications and costs, and could be circumvented by improvements in the area stabilization by using atomic absorption lines, which today reach relative accuracies of $10^{-9}$.

## Errors in Optical Transmission

Given the pulse rate of the laser and strength of attenuation, the mission requirements state that the loss in the optical transmission signal of the femtosecond laser pulses shall not exceed 50 dB. This is in order to collect enough signal photons to generate a statistically significant result.

There are three major sources of transmission loss. The first is the loss due to dispersion within the fibres, which shall be treated separately. The second set of losses are dependent on atmospheric irradiance and interference, and the third upon the altitude of the satellite itself.

## Atmospheric Irradiance and Turbulence

First, we examine the effects of atmospheric turbulence. A wavelength must be selected that is not easily absorbed by the atmosphere, yet is sufficiently developed and standardized for scientific use. As mentioned in the payload description, a 1550 nm wavelength single photon source is readily available on the market, and is one of the few infrared frequencies not greatly absorbed by the atmosphere. Due to the associated high frequency of our emitted photon, ionospheric effects on polarisation angle can be safely ignored. However, Rayleigh scattering through the lower 12km of the atmosphere will cause a beam divergence of 10 $\mu rad$. In an uplink direction this would reduce the signal photons incident on a satellite receiver, as the pre-scattered beam would continue to diverge. A downlink direction would only cause a wide beam divergence in the last 12km of travel and hence more signal photons would reach the receiver. Since the transmission power of a single photon is fixed by the Planck relation, a downlink from satellite to groundstation would be subject to far less transmission loss than an uplink.

Allowing for a pointing error of -2 dB; knowledge of the optical depth of a section of atmosphere, fixing the angle of incidence and using a Monte Carlo method we can estimate the atmospheric transmission loss to about -3 dB [4].

## Establishing a Link Budget

We can modify and simplify the Friis Transmission Equation to give us the following link budget equation [5]:

$$\text{Loss}(dB) = \left[\left(\frac{\pi D_T}{\lambda}\right)\left(\frac{\pi D_R}{\lambda}\right)\left(\frac{\lambda}{4\pi R}\right)\right]^2 L_p L_t, \quad (3)$$

where here $D_T$ is the transmitter diameter, $D_R$ is the receiver diameter, $\lambda$ is the wavelength of the laser (here 1550nm), $R$ is the satellite altitude, $L_p$ is the pointing loss and $L_t$ the transmission loss (taken to be 0.9 and 0.8 respectively, from [4]).

If we assume an apogee of 32000 km and a perigee of 700 km, a ground receiver diameter of 3m, and a satellite transmitter diameter of 0.6m, we calculate a loss in power due to atmospheric turbulence to be -15.43 dB at perigee, and -32.33 dB at apogee. Adding the optical fibre loss of -14.3, we achieve a total loss of -48.62, assuming a safety margin of -2 dB.

Of course, to further reduce signal loss, one could increase the aperture diameters of the receiver and transmitter. However, this causes a loss in manoeuvrability and a significant cost increase for rapidly decreasing returns.

## Signal-to-Noise Ratio

We must also find methods ensuring a signal-to-noise ratio (SNR) greater than 5 dB to produce enough signal data for statistical analysis. It is important to stress that the signal received on Earth is fixed by the link budget above, however since we are trying to detect a single photon out of a plethora of solar and planetary photon noise, optimising our SNR is crucial.

The effects of noise on space to ground quantum channels are well documented [6].

Assuming a downlink, we can express the noise power received by the ground telescope ($P_R$) to be:

$$P_R = H_{SKY} \times \Omega_R \times D_R \times B_{FILTER}, \quad (4)$$

where $H_{SKY}$ is the brightness of the sky in units of $Wm^{-2}Sr\dot{\mu}m$, $\Omega_R$ is the field of view of the telescope in $\mu rad$ and $B_{FILTER}$ is the bandwidth in $nm$.

A time gate filter is also required to ensure that only signal photons are detected. Using atomic clocks on the transmitter and receiver synchronised to 100 ms, a prediction would be made of when the transmitted photon would arrive, in order to trigger the time gate to open at the correct moment. The drawback to this method is that since we are measuring the Shapiro delay in photon arrival time, two separate predictions and thus measurements would have to be taken.

As calculated in [6], using a bandwidth filter of 100 nm, a time gate of 1 ns and assuming clear, nighttime, new moon conditions, we would have to deal with a noise count of $1.25x10^{-5}$ noise photons per second. Inputting this into the standard SNR formula for the worst case (at apogee):

$$\begin{aligned} SNR &= \frac{\text{Signal photons}}{\text{Noise photons}} \\ &= 10\log\left(\frac{4092.6}{1.25\times10^{-5}}\right) \\ &= 85.15dB. \end{aligned} \quad (5)$$

Our resulting SNR is well above the required SNR, which means for descoping purposes one could relax instrument requirements such as telescope aperture diameters at the cost of mission lifetime and statistical accuracy.

## Doppler Shift

The final source of atmospheric error is Doppler shift. This is straightforward to calculate based on the velocity of the satellite. For the worst possible case (at apogee), the Doppler redshift is calculated to be $-62GHz$. This needs to be taken into account at the post-processing stage.

# Mission Design

## Orbit

In order to satisfy scientific requirement **SR2**, data must be taken over a sufficiently large difference in gravitational potential to reach the required confidence of $5\sigma$. An orbit with a perigee of 700 km and an apogee of 32000 km allows the observation of a relativistic time delay of 150 fs; which is both big enough to be resolved by the detectors and still gives a reasonable count rate at maximum altitude.

During the measurement procedure, all other light sources introduce noise. Therefore a measurement at eclipse is desired, but this places severe restrictions on the orbit that render it infeasible. The most feasible alternative is to perform measurements when the ground station is not illuminated by the sun, as the ambient sunlight is enough to wash out the signal from the satellite. For a maximized number of measurements the ground station will be placed close to the poles, to allow consecutive measurements on any orbits for about four months. This placement also guarantees that the satellite will always be tilted away from the sun when pointed toward the ground station, minimizing error from light reflecting off the spacecraft body.

By considering the maximum optical path resulting in a valid measurement, and the movement capabilities of the ground telescope, a connection cone of 45°around the zenith was defined. This allows access times up to 6.4 hours from the northern polar station in Svalbard and 27 minutes from the southern polar station in Troll.

## Launcher

The payload has a total mass of 90kg and therefore a small standard satellite bus can be used to mitigate extraneous costs. After adding the subsystems for attitude and thermal control, the total mass is approximated at 370kg. This weight and the small spacecraft size allows us to use the Vega launcher in order to bring the satellite into a transfer orbit. The four stages of the launcher, with a total of over 120 tonnes of propellant, allows the payload to reach an elliptical orbit with a perigee of 700 km and an apogee of 20 000 km. The spacecraft is then carried to its final orbit by onboard propellant (for details on this, see the section below on spacecraft design).

# Spacecraft Design

## Mass Budget

A simplified mass budget is presented below.

| Subsystem | Mass [kg] | Margin [%] | Mass /w margin [kg] |
|---|---|---|---|
| Instrument | 89.6 | 20 | 107.52 |
| COMMS | 10 | 10 | 11 |
| OBCDH | 1.5 | 10 | 1.65 |
| EPS | 32.79 | 10 | 36.07 |
| Structure | 28 | 20 | 33.6 |
| ADCS | 11.7 | 10 | 12.87 |
| TCS | 14 | 10 | 15.4 |
| Rad. shielding | 50 | 10 | 55 |
| **Total dry mass** | **237.59** | | **273.11** |
| 20 % Tot. margin | 47.52 | | 54.62 |
| **Dry mass /w margin** | **285.11** | | **327.74** |
| Propulsion system: | 78.10 | 20 | 93.72 |
| **Total** | **363.21** | | **421.46** |

## Power Budget

The preliminary spacecraft power budget is presented below. The rightmost column of the table takes the subsystem duty cycle into account.

| Subsystem | Peak power [W] | Average power /w margin [W] | Typical energy per orbit [Wh] |
|---|---|---|---|
| Instrument | 137.3 | 122.76 | 527.87 |
| Attitude Determination and Control System | 382 | 157.5 | 1491.88 |
| Electrical Power System | 30 | 31.5 | 298.38 |
| On-board Command and Data Handling System | 7.3 | 4.4 | 41.68 |
| Communication system | 27 | 27.5 | 0.15 |
| **Total** | **583.6** | **343.66** | **2359.94** |
| System margin (20 %) | 116.72 | 68.73 | 471.99 |
| **Total with margin** | **700.32** | **412.39** | **2831.93** |
| **Spacecraft average power over a typical orbit [W]** | | | **298.97** |

The required electrical power is produced utilizing industry standard space-grade triple junction solar cells. With an surface area of $1m^2$ and typical BOL efficiency of 28% the maximum generated power in BOL is 383 W and 380 W in the end of the 2 year nominal mission.

Two mature battery technologies were considered for the spacecraft operation during eclipse periods and potential anomalous operation modes. The battery system was designed for 5 h of typical operation resulting in capacity requirement of 1500 Wh. Using Ni-$H_2$ batteries with power density of 54 Wh/kg and Depth-of-Discharge of 50% would result in a battery mass of 55.6 kg, while using Li-Ion batteries with power density of 90 Wh/kg and Depth-of-Discharge of 80% reduces

the battery mass to 20.8 kg [7]. Li-Ion batteries are selected for the spacecraft based on this preliminary trade-off.

## RF Communication

Only limited RF communication capability is required since the actual science data is generated on the optical ground station, which tracks, receives and senses the science experiment downlink lasers. However, some RF communications are required for telecommanding the spacecraft and downlinking housekeeping telemetry data.

The telemetry link capacity was sized to be able to downlink the typical housekeeping data amount generated during 1.5 orbits (96 Mbit) in 1 hour (25 kbit/s). Binary Phase Shift Keying (BPSK) with a rate-half convolutional Viterbi forward error correction code was selected to reach a Bit Error Rate (BER) under $10^{-7}$ [8]. This modulation scheme results in downlink transmission rate of 50 kbit/s containing 25 kbit/s of payload data. As the data amount of telecommands is considerably smaller than with the downlink telemetry, an uplink transmission rate of 5 kbit/s containing 2.5 kbit/s of payload data was selected for larger link margin to provide redundancy in potential anomalous operational modes of the spacecraft. A simplified RF budget is shown in the Table below.

| | D/L | U/L | Unit |
|---|---|---|---|
| Tx RF power | 12.04 | 13.01 | dBW |
| Total Tx losses | -0.4 | -2.3 | dB |
| Tx ant. gain | 2.15 | 21.07 | dB |
| Tx ant. pointing loss | -6.75 | -2.21 | dB |
| Total path losses | -177.0 | -177.0 | dB |
| Rx ant. gain | 21.07 | 2.15 | dB |
| Rx ant. pointing loss | -2.21 | -6.75 | dB |
| System T(Noise) | 221 | 614 | K |
| Bitrate | 50000 | 5000 | bits/s |
| **Eb/N0** | **7.00** | **11.63** | **dB** |
| **Required Eb/N0** | **6** | **6** | **dB** |
| Margin | 1.00 | 5.63 | dB |

The proposed system is to use a half-duplex 430 MHz link with proven, high-TRL technologies, whilst keeping the maximum power consumption of the communication system under 28 W on the spacecraft via a low-gain half-wave dipole antenna. Likewise, the RF ground station can be realised with relatively simple equipment and a parabolic antenna with a diameter of only 3 m.

Further analysis has to be performed in order to determine the feasibility of using the 430 MHz UHF band for a bitrate of 50 kbit/s. If allocation of sufficient bandwidth is not possible, utilising S-band frequencies around 2.4 GHz and a directional patch antenna on the satellite shall be considered instead.

## Attitude Determination and Control System

The positioning of the spacecraft is provided by two star trackers. Another is also needed for cold redundancy reasons; the choice of which will be an ASTRO APS system.

This model can work with the moon in its field of view and has the ability to avoid exposure from the Earth and Sun at accpetable angles. THe response time from a “lost in space” situation is below five seconds so control will be readily recovered in the event of loss of contact.

To meet the fine pointing requirements we will use four reaction wheels, taken from the STEREO mission. These will be employed in a pyramidal configuration, working with a LN-200s inertial measurement unit.

One of four reaction wheels will be used for hot redundancy. This unit will be placed near the telescope area and only used to improve the pointing accuracy in extraneous circumstances.

The vibration induced by the reaction wheels will be cancelled using a commercial isolator. The selection of this system depends on laboratory tests. In this test we also have to create a software for the reaction wheels control.

We need two lasers for the tracking system: one on the ground and another in the satellite.

When the satellite enters the field of view, the satellite tracking laser begins to look for the ground laser. When they are locked-on, the tracking algorithm starts.

We need a precision of 6 microradians for this method.

## Onboard Command and Data Handling

The Onboard Command and Data Handling System (OBCDH) controls the system level operation of the JANOS spacecraft. This includes: telemetry and telecommand processing; housekeeping data gathering and processing; and guidance and navigation.

An off the shelf computer, the Cobham Semiconductor Solutions GEN 6 LEON 3FT Single Board Computer (SBC), is proposed as a preliminary solution for the OBCDH system. The ESA-developed LEON 3FT microprocessor architecture is an industry standard solution offering high reliability and adequate computing resources for the JANOS spacecraft. The proposed LEON 3T implementation is certified for up to a total ionizing radiation dose of $10^5$ rad. The SBC includes 64MB of EDAC SRAM Memory, 32 MB

of EDAC Non-Volatile MRAM and has a maximum power consumption 7.3 W while operated at 132 MHz.

### Thermal Control System

In order to achieve the satellite thermal design with reasonable first order estimations, we employed equations for equilibrium temperature distributions. The actual spacecraft will likely exhibit lower maximum temperatures and higher minimum temperatures than those predicted by the equations due to transient effects. Performing a conservative calculation, two situations were considered: the worst hot case scenario (at the 32000 km apogee) and the worst cold case scenario (the spacecraft is subject to periodic eclipse at only 2-3% of the total orbit time, which means a maximum eclipse time of 1 hour). The most critical requirement of the thermal design is the thermal stability of the optical fiber container and for the optical bench. This is accomplished by equipping the satellite with a Multi-Layer Insulation (MLI) coating which is defined by 10 double-sided aluminized layers, separated by Dacron net spacers, with an outer layer of Kapton and silver paint. Another requirement for the thermal control configuration is to maintain an operating temperature range for the instruments and for the electrical parts. This requirement is met by mounting a teflon radiator with an active area of 1.92 $m^2$. Internal heat is redistributed with a system of heat pipes and then dissipated by the radiator. Considering the above mentioned methods for thermal control, the equilibrium temperature of the satellite is stabilised around room temperature; at 24.5 °C.

### Propulsion

To reach the final orbit after separation from the launcher, an additional $\Delta v$ of 323 $ms^{-1}$ is necessary. This will be achieved by an perigee burn with a $400N$ bipropellant thruster. The spacecraft has twelve 10 N thrusters with the capability of moving in 6 a full six degrees of freedom. The thrusters are mounted in pairs on opposite corners and the thrusters facing out of the same side as the telescopes are pointed 45°away to avoid damage to the optical instruments by backscattering of the propellant. The whole propulsion system uses MMH as a propellant and $N_2O_4$ as the oxidizer. At the end of the spacecraft lifetime, another 55 $ms^{-1}$ manoeuvre will lower the perigee down to 200 km, which leads to the burn up of the craft in the atmosphere.

### Radiation and Shielding

The spacecraft's immediate radiation environment, such as fluxes from the solar wind and galactic cosmic rays (GCRs), has a non-negligible effect on the performance of components of the satellite. Therefore, suitable shielding is necessary to ensure the correct operation of the on-board devices. Particular precaution has to be taken for the optical fibre radiation shielding due to the effect of radiation-induced attenuation (RIA), which in this case amounts to 0.5 dB/km for total ionizing dose of 9000 rad. Using aluminium shielding of 1 cm thickness, the radiation dose for 1 year is reduced to 593 rad, which yields an RIA of -1.98 dB. An aluminium shielding of 2 mm is provided for the lasers and the optical bench. This is also ample shielding to guarantee low radiation doses for the remaining optics. The onboard computer needs 1mm aluminium shielding because it can resist up to $10^5$ rad, which is suitably robust for our mission.

## Project Timeline

A schematic of the project timeline is shown in Fig. 4. Phase 0 corresponds to the identification of the different needs and their analysis. During phase A, The feasibility of the mission will be studied. Phase B is a preliminary definition phase. Phase C/D corresponds to the detailed definition, the production and the qualification of the mission systems. Phase E/F begins with the launch, ends with the mission disposal and contains all the mission and science planning, and the data archiving.

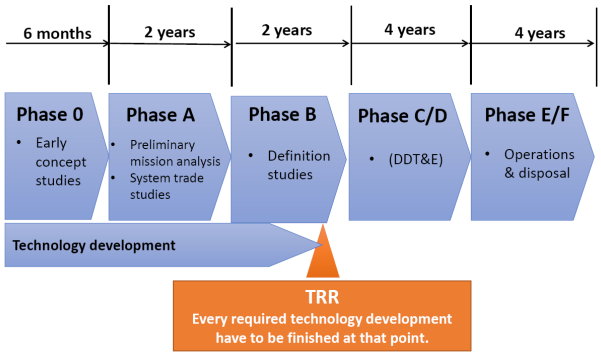


Figure 4: A schematic of the duration of the project phases.

## Cost and Risk Analysis

### Cost Breakdown

Due to the stringent instrument and mission requirements, we can expect the cost of this mission to be fairly high. To ensure high productivity within the project team, we estimate €30M required to cover wages, office infrastructure, and material costs. We can likewise estimate a further €80M for mission and

science operation costs, and a further €50M investment in the development of the required optical fibre technology. To this, we expect €200M in payload costs, mainly for the detector and laser systems; as well as spacecraft and integration costs of €150M. Assuming the standard VEGA launcher rate of €45M and a €28M contingency, we expect our proposed mission to cost €583M. The €250M for development and payload costs would be funded by member states, whilst the remainder would have to be covered by ESA.

## Risk Analysis

To analyze the risks of the mission, we separate the development of the technologies and the operational risks onboard the spacecraft during the mission.

In this analysis, the standard risks for a space mission are not taken into account due to widespread knowledge about them, leaving us more room to explain in depth more specific risks.

The availability of optical fibre cables and the frequency stabilization may not be delayed in the program timeline, as a delay implies that the mission will not be able to progress beyond Phase B. A rushed or incomplete program implies, in turn, that the required safety conditions for a space flight will not be gathered, compromising the entire mission.

One other operational risk is the blackening of fibre cables due to radiation, which poses a significant risk. This process is slowed down due to the aluminum shielding against radiation used in these cables. However, if this blackening process occurs at a higher speed than expected, the mission's duration must be reduced and insufficient data collected. Active avoidance of the van Allen belts by modifying the orbit would mitigate this if needed.

## Conclusion

JANOS will be the first controlled experiment that is capable of unambiguously combining two fundamental foundation stones in modern physics, many of our daily life technologies rely on: Quantum mechanics and General Relativity. Being within the reach of current technology, this experiment might soon satisfy a (long lasting) scientific curiosity. Furthermore it could give rise to improvements in the currently evolving field of free space quantum communication, as well as promote laser and detector technology for space applications.

# References


[1] C. M. Will, "The Confrontation between General Relativity and Experiment," *Living Reviews in Relativity*, vol. 9, 2006.

[2] M. Zych, F. Costa, I. Pikovski, T. C. Ralph, and C. Brukner, "General relativistic effects in quantum interference of photons," *Classical and Quantum Gravity*, vol. 29, p. 224010, Nov. 2012.

[3] L. Shen, W.-P. Huang, G. Chen, and S. Jian, "Design and optimization of photonic crystal fibers for broad-band dispersion compensation," *IEEE Photonics Technology Letters*, vol. 15, pp. 540–542, Apr. 2003.

[4] Y. M. Timofeyev and A. V. Vasilev, *Theoretical Fundamentals of Atmospheric Optics*. Cambridge Int Science Publishing, 2008.

[5] J. A. Shaw, "Radiometry and the Friis transmission equation," *American Journal of Physics*, vol. 81, p. 33, Jan. 2013.

[6] M. Er-long, H. Zheng-fu, G. Shun-sheng, Z. Tao, D. Da-sheng, and G. Guang-can, "Background noise of satellite-to-ground quantum key distribution," *New Journal of Physics*, vol. 7, pp. 215–215, Oct. 2005.

[7] P. Fortescue, G. Swinerd, and J. Stark, *Spacecraft Systems Engineering*. 2011.

[8] W. J. Larson and J. R. Wertz, *Space mission analysis and design*. 1992.


# Appendices

## Appendix A: Correction due to Relatistic Motion of the Orbiter

In the presence of a gravitational field from a body of mass $M$, the time dilation due to general relativity is

$$t_0 = t_f \frac{1}{\sqrt{1 - \frac{2GM}{r \cdot c^2}}}, \tag{6}$$

where $t_0$ is the time far from the gravitational source, $t_f$ is the time within the field, $G$ is Newton's gravitational constant, $r$ is the distance to the centre of mass of the body, and $c$ is the speed of light. For a weak field, such as close to Earth, a first order expansion of (6) is

$$t_0 = t_f \left(1 + \frac{2GM}{rc^2}\right). \tag{7}$$

In our case, the time difference between photons passing through fibres of length $l$ at Earth's surface (radius $r_0$), and at a height $h$ above the surface, respectively, is measured. Using (7), this is

$$\Delta\tau_{GR} = \frac{2GMln}{c^3}\left(\frac{1}{r_0} - \frac{1}{r_0 + h}\right), \tag{8}$$

where $n$ is the refractive index. Here, $l = 60$ km and $n = 1.5$, $\frac{ln}{c} = 0.3$ ms.

For a complete description, one also has to take into account special relativity, since the spacecraft is moving. Since the gravitational field is weaker at the spacecraft than at Earth, these two effects will counteract each other. The time dilation for an object moving at speed $v$ is

$$t = \frac{t'}{\sqrt{1 - \frac{v^2}{c^2}}} \approx t' \left(1 + \frac{v^2}{2c^2}\right) \tag{9}$$

if $v << c$, where $t$ is the proper time of the stationary object and $t'$ is the proper time of the moving object. For a spacecraft orbiting Earth, the orbital speed is

$$v_r = \sqrt{\frac{GM}{r_0 + h}}. \tag{10}$$

To obtain the relative speed $v$, one needs to subtract the rotational velocity of Earth at the ground station $\mathbf{v_0} = v_0 \mathbf{e}_\phi$, so

$$v = |\mathbf{v_r} - \mathbf{v_0}|. \tag{11}$$

Therefore, the time dilation from special relativity is

$$\Delta\tau_{SR} = \frac{ln}{c} \frac{|\mathbf{v_r} - \mathbf{v_0}|}{2c^2}, \tag{12}$$

and consequently the total time dilation is

$$\Delta\tau = \frac{nl}{c} \frac{|\mathbf{v_r} - \mathbf{v_0}|}{2c^2} - \frac{2GMln}{c^3} \left(\frac{1}{r_0} - \frac{1}{r_0 + h}\right). \tag{13}$$

For orbits where $v_0 << v_r$, (13) can be simplified as

$$\Delta\tau = \frac{GMnl}{c^3} \left(\frac{3}{2} \frac{1}{r_0 + h} - \frac{1}{r_0}\right). \tag{14}$$

This is the modification to the Shapiro delay due to the special relativistic motion of the orbiter.